Results in Engineering 27 (2025) 106926

Contents lists available at ScienceDirect

Results in Engineering

journal homepage: www.sciencedirect.com/journal/results-in-engineering

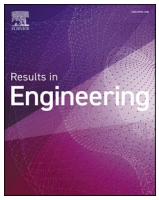

Research paper

Adsorption of tetracycline using silica nanoparticles: a comparative study of sodium silicate-derived and fly ash-derived silica nanoparticles

Eric E. Houghton, Litha Yapi, Shepherd M. Tichapondwa *

Water Utilization and Environmental Engineering Division, Department of Chemical Engineering, University of Pretoria (UP), Pretoria 0002, South Africa

ARTICLE INFO

Keywords:
Fly ash
Adsorption
Tetracycline
Silica nanoparticles

ABSTRACT

Fly ash (FA), a fine particulate residue produced from the combustion of coal in thermal power plants, is generated in substantial quantities and presents significant challenges related to its environmental management and disposal. Repurposing FA can mitigate waste accumulation while contributing to sustainable environmental solutions. One promising approach is utilising FA as an adsorbent for removing pollutants from aqueous solutions, particularly emerging contaminants (ECs).

In this study, silica nanoparticles were synthesised from FA (FA-SiNPs) and subsequently modified with iron to produce Fe-SiNPs. As a control, silica nanoparticles were synthesised directly from a sodium silicate solution (SSSNPs). The different silica nanoparticles were used as adsorbents to remove tetracycline (TC) from aqueous solutions under identical conditions, to compare their adsorption performance. Under the identical conditions, Fe-SiNPs demonstrated superior performance, achieving 59 % removal of TC, compared to 30 % and 20 % removal by FA-SiNPs and SSSNPs, respectively. The enhanced adsorption capacity of Fe-SiNPs was attributed to the presence of iron, which facilitated TC removal through chelation. Upon optimisation of experimental parameters, a maximum TC removal efficiency using Fe-SiNPs of 86 % was observed at the optimal dosage of 5 g/L within a pH range of 4 to 5. The adsorption kinetics were best described by the Elovich model, whereas the equilibrium data fitted the Langmuir isotherm model with a maximum adsorption capacity of 32.31 mg/g at 30 °C. Thermodynamic analysis revealed that the adsorption process was both spontaneous and exothermic in nature. The adsorption of TC on Fe-SiNPs involved chemisorption, electrostatic attraction and hydrogen bonding. This study highlights the potential of FA-derived silica nanoparticles, particularly Fe-SiNPs, as cost-effective and sustainable adsorbents for TC removal from contaminated water.

1. Introduction

Water is a limited yet essential resource for all living organisms [1]. However, its availability is increasingly threatened by pollution, which poses severe risks to both human health and the environment [2]. Among the various pollutants, emerging contaminants (ECs), such as endocrine-disrupting chemicals (EDCs), pharmaceuticals and personal care products (PPCPs), have gained significant attention due to their persistence in the environment and high toxicity to microorganisms [3]. Tetracycline (TC) is a known emerging contaminant and one of the most commonly used antibiotics in human and veterinary medicine [4]. More than 70 % of tetracycline antibiotics are excreted from the body either in their unmetabolized form or as active/inactive metabolites [5]. Wastewater treatments that rely on biological processes are ineffective at degrading tetracycline and its metabolites. Thus, TC may be persistent in the wastewater system and disrupt the activated sludge treatment system of wastewater treatment plants. As a result, tetracycline can enter the aquatic environment through the direct discharge of effluents from wastewater treatment plants [6].

The presence of tetracycline in the environment can promote the development of antibiotic-resistant bacteria which is detrimental to human and animal health. Additionally, TC has a long-term persistence in the environment, due to its high chemical stability [7]. There are various treatments methods available for the removal of tetracycline from aqueous solutions including, photocatalytic degradation, adsorption, membrane separation, ozonation, phytoremediation [4]. Adsorption stands out as an environmentally friendly and efficient method, offering several advantages, including low energy consumption and minimal maintenance costs [8]. Many commercial adsorbents, such as activated carbon and graphene, are highly efficient but can be costly [9].

* Corresponding author.
E-mail address: shepherd.tichapondwa@up.ac.za (S.M. Tichapondwa).

https://doi.org/10.1016/j.rineng.2025.106926
Received 29 July 2025; Accepted 24 August 2025
Available online 25 August 2025

Alternatively, low-cost adsorbents sourced from industrial waste, such as coal fly ash, and agricultural waste, including sugar beet pulp and rice husk, provide a more economical and sustainable alternative [10].

Fly ash (FA) is a solid by-product generated from coal combustion for electricity production. In 2015, approximately 750 million tonnes of FA were produced, yet only about 25 % of the total generated FA was utilized [11]. Fly ash is considered as a hazardous material as it contains various heavy metals, such as lead (Pb), cadmium (Cd), mercury (Hg), molybdenum (Mo) [12]. Consequently, FA that is not utilised must be stored in dry specialised landfills or in ash ponds [13,14]. Dry disposal of fly ash requires a large area which may not be readily available and will incur high costs [15]. Ash ponds can reduce the amount area required but if they are inadequately lined, the toxic elements present in the fly ash can leach out and contaminate groundwater aquifers [16].

The sol-gel method is one of the simplest and most efficient approaches for synthesizing silica nanoparticles (SiNPs) [17]. However, conventionally used silica precursors for sol-gel methods such as tetramethyl orthosilicate (TMOS) and tetraethyl orthosilicate (TEOS) are expensive [18]. The large silica content in fly ash can be utilised as a silica precursor for the production of silica nanoparticles (SiNPs) [19,20]. Leveraging fly ash as a low-cost silica source not only supports waste valorisation but also promotes more sustainable and economically viable silica nanoparticle production. Aphane, Doucet [20] estimated that the use of one tonne of FA can yield approximately $33 million worth of silica nanoparticles, highlighting the significant economic potential of fly-ash derived silica nanoparticles. Beyond economic value, SiNPs are also effective adsorbents due to their stable structure, hydrophilic nature, and large surface area. The adsorption efficiency of SiNPs can be further enhanced through surface modification [21]. Iron modification, in particular, has been shown to introduce active sites that facilitate surface complexation between TC molecules and iron on the surface of SiNPs, thereby significantly increasing the adsorption capacity [22,23].

A SCOPUS database search using the keywords 'Coal fly ash,' 'Silica Nanoparticles,' and 'Adsorption' yielded only 12 relevant publications. However, none of these studies explored the use of fly ash silica nanoparticles to remove emerging contaminants, particularly tetracycline. The study addresses this notable gap and explores the adsorption interactions between TC and SiNPs. This work is an extension on recent work surrounding coal fly ash waste valorisation [24].

This study aims to demonstrate that fly ash may be used to synthesize silica nanoparticles that can be effective in the removal of tetracycline from water and wastewater. In addition to FA-SiNPs, iron modified fly ash silica nanoparticles (Fe-SiNPs) were synthesised and as a comparator, sodium silicate derived silica nanoparticles (SSSNPs) were also synthesised. These nanoparticles were then characterised using XRD, XRF, BET, SEM and tested comparatively, focusing on Fe-SiNPs adsorption efficiency under varying conditions.

2. Materials and methods

2.1. Materials

Tetracycline (TC) was procured from Sigma-Aldrich, located in Steinheim, Germany. Fly ash (FA) was collected from Matla Power Station, situated in Kriel, Nkangala District, Mpumalanga Province, South Africa. Sodium hydroxide (NaOH) pellets, Hydrochloric acid (HCl, ~32 %), and ferric chloride hexahydrate ($FeCl_3{\cdot}6H_2O$) were obtained from Glassworld, South Africa. Deionised (DI) water used throughout this study was produced using an Elga Purelab purification system. was supplied by an Elga Purelab Chorus unit. Filtration was carried out using qualitative-grade Whatman No 40 filter paper, featuring a pore size of 8 μm.

2.2. Preparation of silica nanoparticles derived from fly ash (FA-SiNPs)

Sodium silicate was initially synthesised from the fly ash using the sequential acid–alkaline leaching (SAAL) method reported by Aphane, Doucet [20]. Hydrochloric acid leaching was used to reduce the alumina in the fly ash. Subsequently, sodium hydroxide was used to extract silica from the purified FA. Specifically, 10 g FA was used with 100 ml of a 10 M HCl solution for the acid leaching. The mixture was magnetically stirred and heated under reflux conditions. A stirrer speed of 300 rpm, with a duration of 4 h and a temperature of 95 °C, was used to leach out the alumina from the FA. The acid leachate phase was then separated with centrifuging for 20 min at a temperature of 4 °C and a speed of 9000 rpm. The remaining FA was washed once and dried overnight at 60 °C.

The FA extract recovered after acid leaching (approx. 7.5 g) was immersed in 100 ml of a 10 M NaOH solution. The mixture was then suspended in a silicone bath on a magnetic stirrer for a duration of an hour at a temperature of 95 °C, and a stirrer speed of 300 rpm. Using filter paper, the leachate (sodium silicate) was separated from the solid residue. The resulting sodium silicate solution (approx. 70–80 ml) was added to 20 ml of a 3 w/w % polyethylene glycol (PEG) solution. A LABOTEC ultrasonic water bath was used to first sonicate the PEG solution for 30 min at 55 °C prior to use. Subsequently, the sodium silicate solution was added slowly to the PEG solution while in an ultrasonic water bath (55 °C, 20 Hz).

The PEG-sodium silicate solution was slowly titrated with 5 M HCl to a pH of 4. After titration, the visible gel solution was left to sonicate for 30 min. The gel solution was then covered and left to age overnight. The gel solution was centrifuged for 20 min at 4 °C and 9 000 rpm. The recovered gel was washed several times to remove Na^+ and Cl^- ions. Silver nitrate ($AgNO_3$) was used to test the presence of Na^+ and Cl^- ions. If no AgCl precipitate was observed in the supernatant of the wash water, the washing was deemed to be complete. The final product was calcined at 650 °C for 2 h.

An aliquot of 5 g of the synthesised silica nanoparticles was added to 250 ml of 1 M HCl and stirred on a magnetic stirrer for 3 h at 110 °C and 300 rpm under reflux conditions. The resulting nanoparticles were centrifuged for 20 min at 4 °C and 9 000 rpm and calcined at 400 °C for 2 h. The product was denoted as FA-SiNPs.

2.3. Preparation of iron-modified silica nanoparticles (Fe-SiNPs) from FA-SiNPs

The iron impregnation synthesis method was adopted from Kiprono, Kiptoo [25]. This entailed adding 5 g of FA-derived silica nanoparticles to 25 ml of a 74 mM $FeCl_3{\cdot}6H_2O$ solution. The pH of the mixture was then adjusted to 7 and then stirred on a shaking table for a duration of an hour at 250 rpm and room temperature. Afterwards, the solution was centrifuged for 20 minutes at 4 °C and 9 000 rpm, washed twice, and left to dry overnight at 60 °C. Finally, the resulting powder was calcined for 6 h at 500 °C. The product was denoted as Fe-SiNPs.

2.4. Preparation of silica nanoparticles derived from sodium silicate solution (SSSNPs)

The silica nanoparticles synthesis from sodium silicate solution was a variation of the synthesis from the fly ash. 5 ml of sodium silicate was diluted with 95 ml of DI water and the solution was stirred using a magnetic stirrer placed in a silicone oil bath for 1 h at 95 °C and 300 rpm. Note that the synthesis follows the exact same steps shown in the preparation of FA-SiNPs, from the addition of the sodium silicate to the PEG solution to the calcination. Note there was no post acid purification required. Fig. 1 presents a scheme of experiments for the adsorbents.

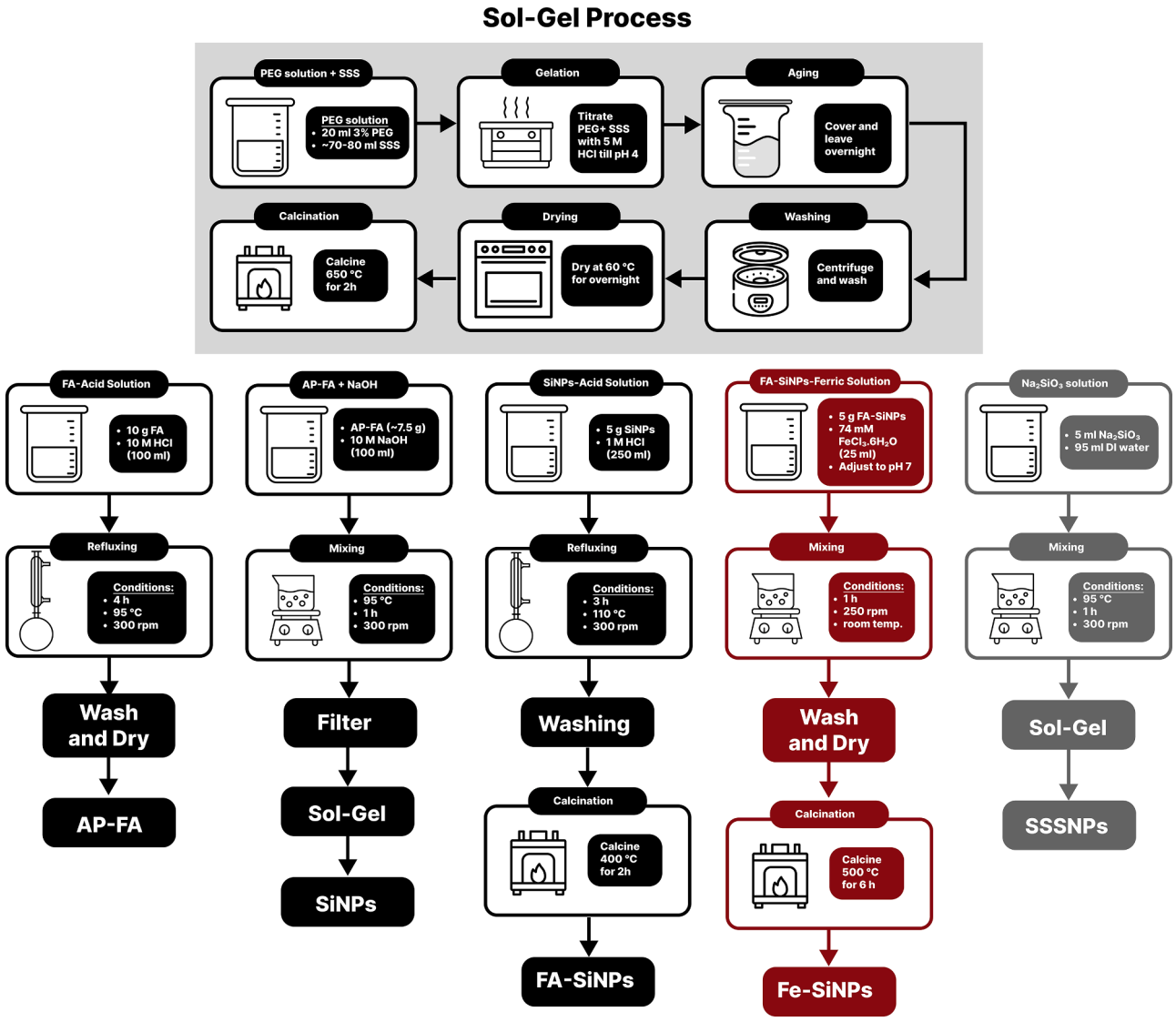

Fig. 1. Scheme of experiments for the adsorbents.

2.5. Adsorption experiments

Preliminary adsorption tests were conducted with FA-SiNPs, SSSNPs, and Fe-SiNPs to compare and identify the most effective adsorbent for TC removal. Based on the outcomes of preliminary tests, the rest of the experiments were then carried out with Fe-SiNPs. The experimental parameters employed in the adsorption studies are summarized in Table 1.

Table 1
Summary of the conditions and parameters used in the Fe-SiNPs adsorption experiments.

Study Type	Adsorbent(s) used	Key parameters			
		Co (ppm)	Ph	Dosage (g/L)	Time (h)
Initial Screening	FA-SiNPs, SSSNPs, Fe-SiNPs	100	5	5	0.5
Dosage effect	Fe-SiNPs	50	5	1–10	2
pH effect	Fe-SiNPs	70	2–9	5	2
Kinetics	Fe-SiNPs	70	5	5	–
Isotherms	Fe-SiNPs	90–140	5	5	6
Thermodynamics study	Fe-SiNPs	Temperature: 30 °C, 40 °C, 50 °C			

Batch adsorption experiments were performed in triplicates with the results shown being the mean of the triplicates. A 200-ppm tetracycline stock solution was diluted with deionized water to prepare the experimental solutions. All adsorption experiments were conducted in triplicates and the results shown are the mean of the triplicates. An orbital shaking table operating at 250 rpm was used to agitate the samples. After each experiment, a 2 mL sample was centrifuged at 10 000 rpm for one minute to isolate the adsorbent, and the TC concentration was analysed from the resulting supernatant. A 1:1 dilution of the supernatant was performed with 0.1 M NaOH before analysis. At elevated pH levels, TC predominantly exists in its dianionic form (TC^{2-}), which exhibited an intensified yellow colour, enhancing detection via UV–Vis spectrophotometry. A VWR UV-1600 PC spectrophotometer in a scanning range of 500 nm to 300 nm at 1 nm intervals was used from determine the initial and final TC concentrations. Note that absorbance at peak wavelength of 381 nm was used to develop the calibration curve.

2.6. Adsorbent characterization

X-ray diffraction (XRD) analysis was performed using a PANalytical X'Pert Pro system in θ-θ geometry, featuring an X'Celerator detector. The instrument employed variable divergence slits, fixed receiving slits, and Co-Kα radiation (λ=1.789 Å) filtered through an Fe filter. X'Pert

Highscore plus software was utilized to determine the mineralogy of the samples by matching diffraction pattern of the sample with the ICSD database. X-ray fluorescence (XRF) spectroscopy was performed using a Thermo Fisher ARL Perform'X sequential XRF spectrometer equipped with Uniquant software. The specific surface area was determined by nitrogen physisorption at 77.35 K using a Micromeritics TriStar II analyzer. Prior to measurements, samples were degassed under vacuum at 110 °C for 18 h. SEM analysis was conducted on a Zeiss Crossbeam 540 FEG SEM instrument to evaluate the morphology of the synthesized materials. The instrument used an Oxford instruments detector and Aztec 3.0 software SP1. Samples for SEM analysis were carbon coated prior to analysis with a SEM auto-coating unit E2500 (Polaron Equipment Ltd).

Fig. 2

3. Results and discussion

3.1. XRD analysis

The XRD analysis focuses on the crystallinity of the silica nanoparticles. The XRD patterns for FA-SiNPs, SSSNPS, and Fe-SiNPs are shown in Fig. 3. None of the materials exhibit sharp peaks but only a single broad peak centred at $2\theta = 25^{\circ}$, this indicates the amorphous nature of the materials [26]. There was also no observable change in crystallinity due to the modification of FA-SiNP to form Fe-SiNPs.

3.2. XRF analysis

The chemical composition of FA-SiNPs, SSSNPs, and Fe-SiNPs is shown in Table 2. Both FA-SiNPs and SSSNPs had a high silicon content, exceeding 90 wt %, indicating the successful synthesis of silica-rich nanoparticles. FA-SiNPs contained 94.45 wt % SiO_2 with trace amounts aluminium (0.14 wt %) and titanium (0.07 wt %), most likely originating of the FA precursor. In contrast, SSSNPs, synthesized from pure sodium silicate, demonstrated a silica content of 91.83 wt % and showed virtually no impurities. While FA can serve as a viable precursor for the synthesis of high-silica-content nanoparticles, the need for extensive acidic treatment to eliminate impurities presents a drawback when compared to the synthesis from chemical-grade sodium silicate. Fe-SiNPs, synthesised through iron modification of FA-SiNPs, showed a notably 1.91 % iron content, confirming successful iron modification.

3.3. Surface area and morphology analysis

The SEM images of FA-SiNPs, SSSNPs, and Fe-SiNPs are displayed in Fig. 4. The surface morphology of all adsorbents is characterized by spherical particles with sizes of $\leq$ 200 nm. Notably, the morphology

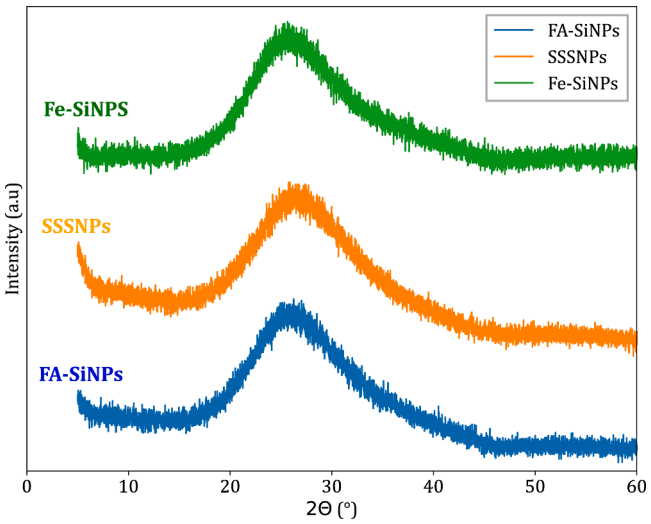

Fig. 3. XRD Patterns for FA-SiNPs, SSSNPS, and Fe-SiNPs.

remained unchanged following iron modification.

Table 3 summarizes the specific surface areas of FA-SiNPs, SSSNPs, and Fe-SiNPs as determined by BET analysis. Among these, SSSNPs exhibited the highest specific surface area of 305 m^2/g, while FA-SiNPs had a specific surface area of 140 m^2/g, which is approximately half that of SSSNPs. As depicted in Fig. 4, FA-SiNPs formed large agglomerates of nanoparticles, in contrast to SSSNPs. This agglomeration reduces the available interfacial area, thereby decreasing the surface area [27]. The formation of large agglomerates in FA-SiNPs synthesis could be attributed to the presence of impurities, primarily aluminum and iron. These impurities may act as coagulating agents, promoting excessive coagulation of colloidal silica, which leads to the development of large agglomerates. This underscores the importance of the pre-acidic treatment during the synthesis process as it could impact the surface area of the synthesised FA-SiNPs. The specific surface area of Fe-SiNPs was lower than that of the parent FA-SiNPs, likely due to the loading of iron oxide onto the surface of FA-SiNPs [28].

3.4. Comparative evaluation of adsorbents for tetracycline (TC) removal

Initial adsorption screening of FA-SiNPs, SSSNPs, and Fe-SiNPs was conducted under identical experimental conditions to assess their comparative performance for tetracycline removal. The percentage removals of TC for FA-SiNPs, SSSNPs, and Fe-SiNPs are shown in Fig. 5. FA-SiNPs and SSSNPs demonstrated relatively low percentage removals, at 30 % and 20 %, respectively. The slightly higher percentage removal

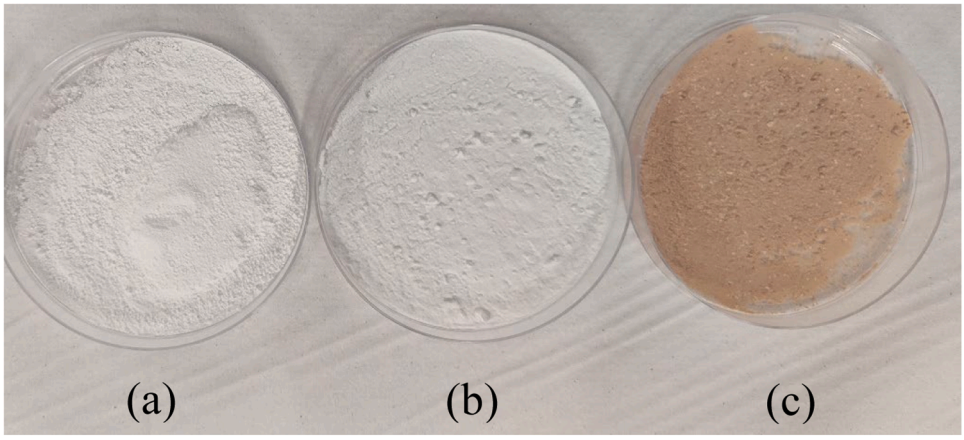

Fig. 2. Synthesised materials - (a) SSSNPS, (b) FA-SiNPs, and (c) Fe-SiNPs.

Table 2
Chemical composition of FA-SiNPs, SSSNPs, and Fe-SiNPs.

Oxides (wt %)	SiO_2	Al_2O_3	Fe_2O_3	Na_2O	K_2O	P_2O_5	MgO	TiO_2	CaO	CuO	LOI*
FA-SiNPs	94.45	0.14	0.01	0.05	0	0	0.03	0.07	0.01	0	5.23
SSSNPs	91.83	0	0.02	0.02	0	0.02	0.02	0.01	0.01	0	8.06
Fe-SiNPs	91.38	0.55	1.91	0.56	0.1	0.09	0.08	0.07	0.03	0.02	5.19

LOI* - Loss on Ignition.

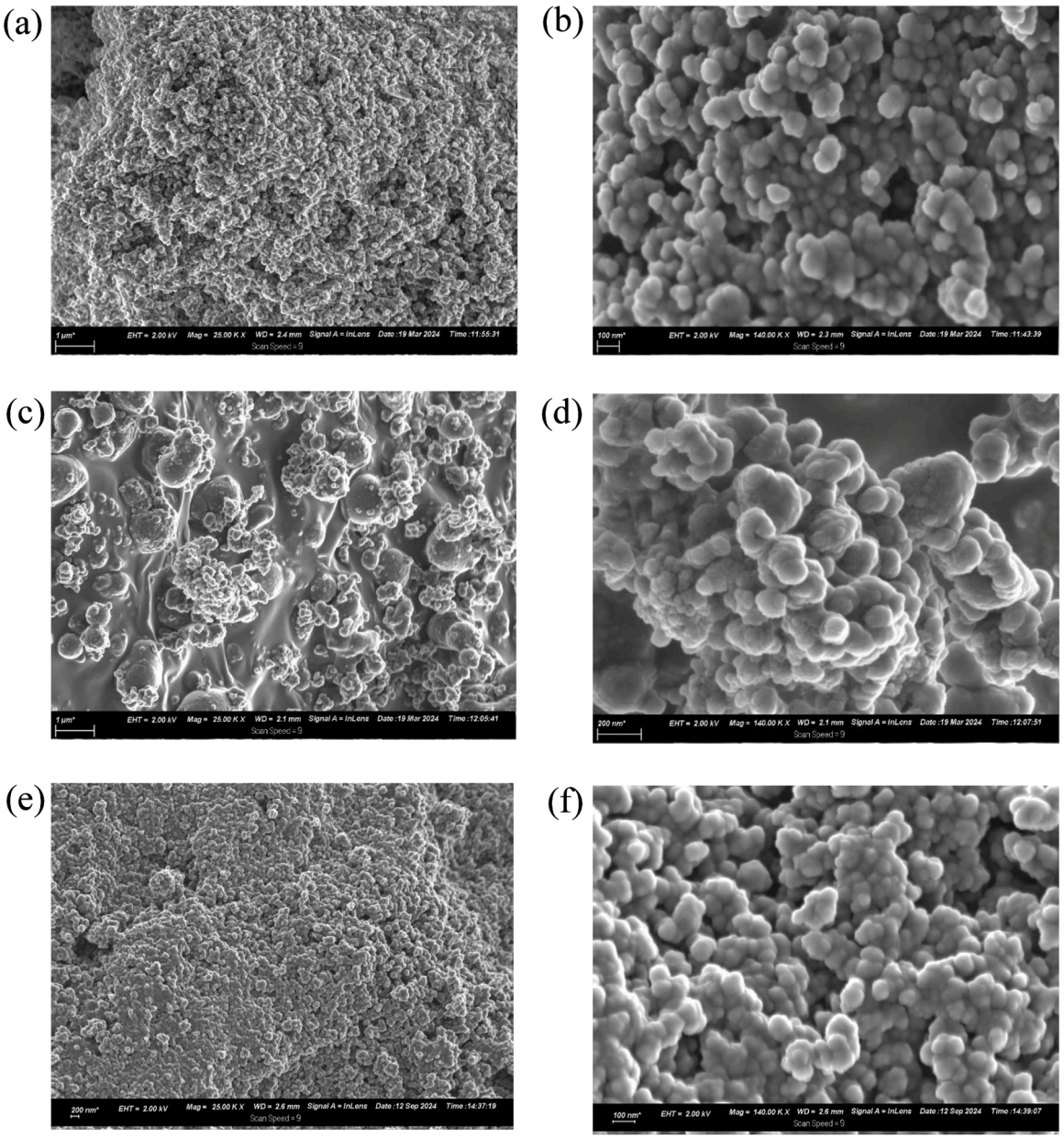

Fig. 4. SEM images for (a & b) FA-SiNPs, (c & d) SSSNPs, and (e & f) Fe-SiNPs. Note that the magnification for (a), (c), (e) is 25 000 and for (b), (d), (f) is 140 000.

Table 3
Specific surface area for FA-SiNPs, SSSNPs, and Fe-SiNPs using BET method.

Material	FA-SiNPs	SSSNPs	Fe-SiNPs
Specific surface area (m^2/g)	140.6	305	110.83

observed for FA-SiNPs was attributed to the presence of small impurities, such as aluminum.

Fe-SiNPs had the highest percentage removal at 59 %. The high percentage removal was attributed the presence of iron in Fe-SiNPs. Zhang, Lan [22] observes that the adsorption characteristics of TC can be improved by the presence of iron in the adsorbent, owing to surface complexation between TC, a chelating agent, and iron. Note that all further adsorption studies carried out were conducted with Fe-SiNPs.

3.5. The effect of adsorbent dosage

Fig. 6(a) shows the effect of the adsorbent dosage of Fe-SiNPs on the

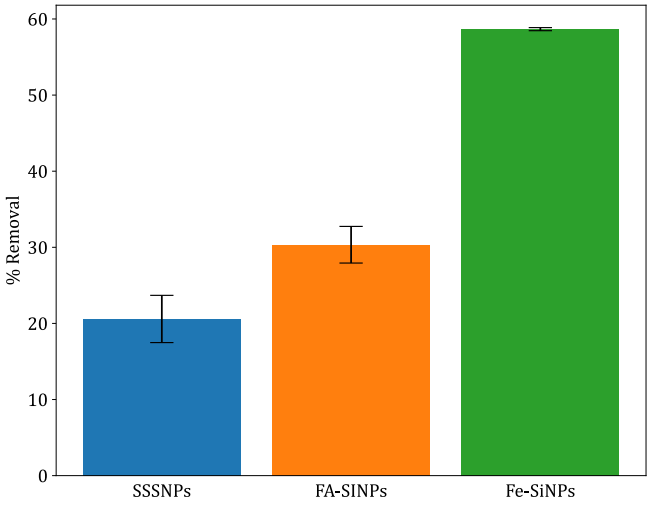

Fig. 5. The TC removal efficiency achieved with FA-SiNPs, SSSNPs, and Fe-SiNPs under the following conditions – pH: 5, Dosage: 5 g/L, Co: 100 ppm, contact time: 0.5 h.

removal of TC. Increasing the dosage of Fe-SiNPs increased the percentage removal of TC. However, after a dosage of 5 g/L, the increase in percentage removal was marginal, at only about 5 %. Therefore, 5 g/L was the optimal dosage, as there was no substantial increase in the percentage removal of TC after a dosage of 5 g/L.

3.6. The effect of pH

Fig. 6(b) shows the effect of pH on the removal of TC on Fe-SiNPs. Fig. 7(a) presents the speciation profile of tetracycline and Fig. 7(b) shows the zeta potential of Fe-SiNPs over various pHs. The maximum percentage removal was observed at pHs 4 and 5; therefore, the optimal pH was 4 - 5. At the optimized dosage and optimized pH range, the maximum TC removal using Fe-SiNPs was 86 %. At pHs of 4 - 5, TC is neutral while Fe-SiNPs is negatively charged. At pHs of 4 - 5, TC can be absorbed as a cationic species. This suggests there is an electrostatic attraction at pHs 4 and 5. Tetracycline adsorption declined at pH values below 4, where TC predominantly exists in its cationic form and the Fe-SiNPs surface becomes less negatively charged, thereby weakening electrostatic attraction. Similarly, at pH values above 5, adsorption efficiency also decreased due to the anionic nature of TC and the negatively charged surface of Fe-SiNPs, resulting in electrostatic repulsion that hinders adsorption. Zhang, Lan [22] utilised amino-Fe (III) functionalized SBA15 to adsorb TC and similarly observed an optimal pH around 4–5, attributed to the amphoteric nature of TC.

3.7. Adsorption kinetics study

Nonlinear regression was used to model the adsorption kinetic models. The pseudo first order model (PFO), pseudo second order model (PSO), Elovich model and the Langmuir kinetic model, presented in Eqs. (1), (2), (3) and (4), were used to describe the adsorption kinetics [29]:

$$q_t = q_e\left(1 - e^{-k_1 t}\right) \tag{1}$$

$$q_t = \frac{k_2 q_e^2 t}{1 + k_2 q_e t} \tag{2}$$

$$q_t = \frac{1}{\beta}\ln\left(1 + \alpha\beta t\right) \tag{3}$$

$$\frac{dq_t}{dt} = k_a C_t\left(1 - \frac{q_t}{q_{max}}\right) - k_d\frac{q_t}{q_{max}} \tag{4}$$

where k_1(1/min) and k_2 (g/(mg·min) represent the rate constants for the PFO and PSO, q_{max} (mg/g) denotes the maximum adsorption capacity constant, α is initial adsorption rate (mg·g^{-1}·min^{-1}); β is the adsorption/desorption constant (g/mg), k_a (L/g/min), k_d (mg/L/min) correspond to the adsorption and desorption rate constants for the Langmuir kinetic model. The kinetic parameters for the adsorption of TC in Fe-SiNPs are shown in Table 4.

3.8. Adsorption isotherms

Similarly, nonlinear regression was used to model the adsorption isotherms. The Langmuir isotherm model, Freundlich isotherm model, and the Temkin isotherm model, given in Eqs. (5), (6), and (7), were used to describe the adsorption isotherms [30]:

$$q_e = \frac{q_m K_L C_e}{1 + K_L C_e} \tag{5}$$

$$q_e = K_f C_e^{\frac{1}{n}} \tag{6}$$

$$q_e = B_T \ln\left(A_T C_e\right) \tag{7}$$

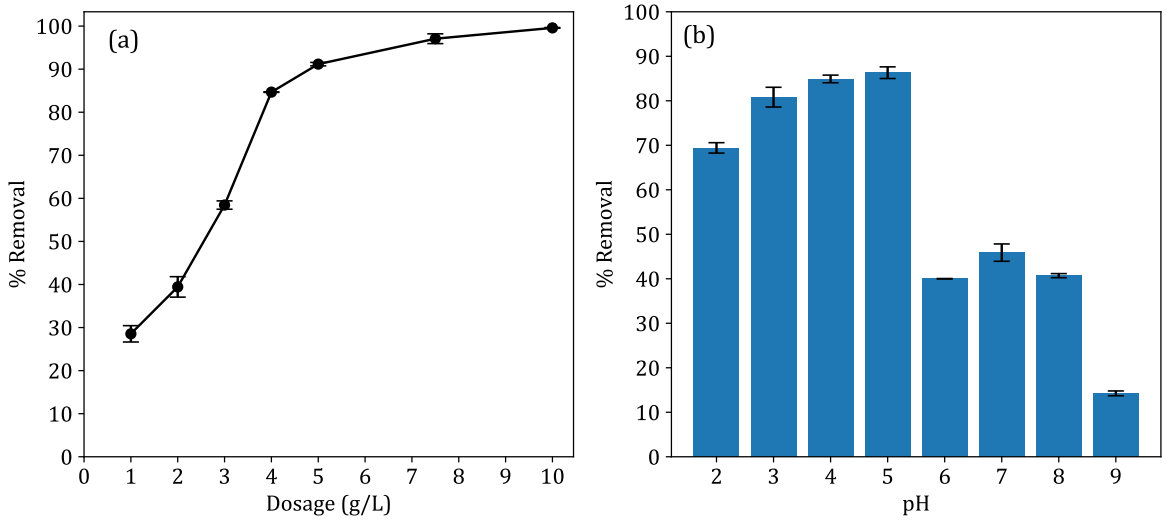

Fig. 6. (a) % Removal of TC versus adsorbent dosage (conditions – pH: 5, Co: 50 ppm, contact time: 2 h), and (b) % Removal of TC versus pH (conditions – Dosage: 5 g/L, Co: 70 ppm, contact time: 2 h).

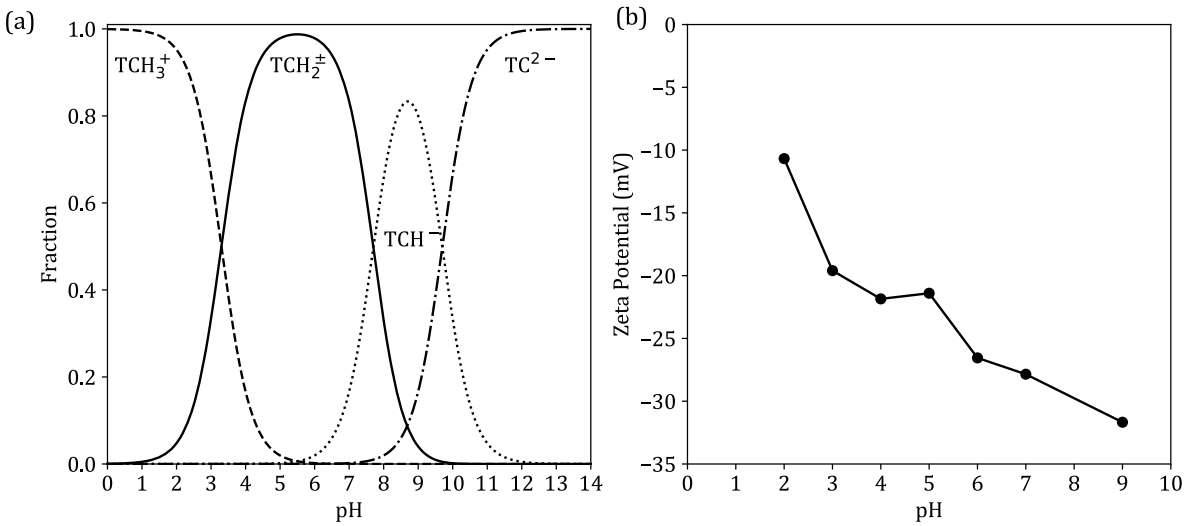

Fig. 7. (a) Speciation profile of tetracycline and (b) zeta potential of Fe-SiNPs at various pHs.

Table 4
Kinetic model parameters and associated statistical metrics for tetracycline adsorption.

Kinetic Model	Kinetic Parameters		Statistical Parameters	
PFO	q_e (mg/g)	14.78	SE	37.51
	k_1 (1/min)	0.19	R^2	0.84
PSO	q_e (mg/g)	15.36	SE	16.91
	k_2 (g/mg/min)	0.03	R^2	0.93
Elovich	α (mg/g/min)	78.69	SE	0.89
	β (g/mg)	0.55	R^2	0.996
Langmuir kinetic	k_a (L/g/min)	0.053	SE	20.91
	k_d (mg/L/min)	0	R^2	0.91
	q_{max} (mg/g)	15.25		

SE - Squared Error.

where q_m (mg/g) represents the maximum adsorption capacity; K_L (L/mg) is the Langmuir constant; K_f is the Freundlich isotherm constant (mg/g), n denotes the adsorption intensity, B_T (J/mol) Temkin constant related to heat of sorption, and A_T (L/mg) is Temkin equilibrium binding constant. The adsorption isotherms of TC on Fe-SiNPs at 30 °C, 40 °C and 50 °C fitted with all the isotherm models are presented in Fig. 8

Table 5 summarizes the parameters and statistical metrics associated with each adsorption isotherm model. The Langmuir isotherm model exhibited the lowest squared error and highest R^2 values across all temperatures except at 40 °C, indicating it most accurately describes the tetracycline adsorption isotherms. This superior fit implies that tetracycline adsorption onto Fe-SiNPs predominantly occurs via monolayer coverage on a homogeneous surface [31]. Table 6 presents the maximum adsorption capacities (q_m) of similar adsorbents to Fe-SiNPs for tetracycline removal.

3.9. Adsorption thermodynamics study

The Gibbs free energy (ΔG°) was calculated using to Eq. (8), while the entropy change (ΔS°) and enthalpy change (ΔH°) were derived from the linear van Hoff's equation shown in Eq. (9). The dimensionless constant, K_{eq}, was determined from the Langmuir constant, K_L, according to Eq. (10).

$$\Delta G^\circ = -RT\ln(K_{eq}) \tag{8}$$

$$\ln(K_{eq}) = \frac{\Delta S^\circ}{R} - \frac{\Delta H^\circ}{RT} \tag{9}$$

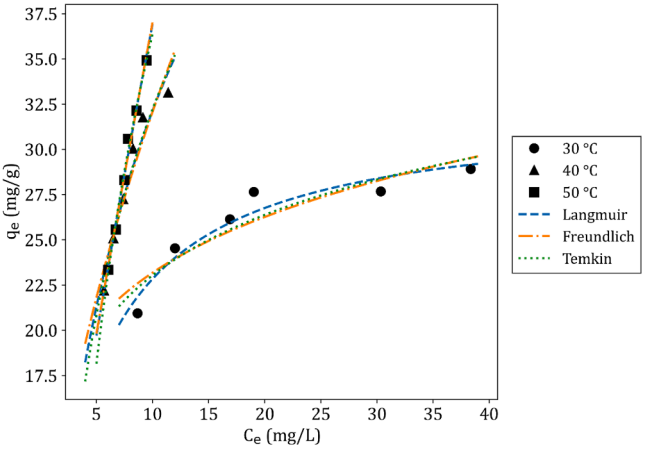

Fig. 8. Adsorption isotherms of TC on Fe-SiNPs at 30 °C, 40 °C, and 50 °C were fitted using Langmuir, Freundlich, and Temkin models under the following experimental conditions: pH 5, adsorbent dosage 5 g/L, and contact time of 6 hours.

$$K_{eq} = K_L \times 1000 \times M_w \times \frac{C^\circ_{Absorbate}}{\gamma_{Absorbate}} \tag{10}$$

where T (K) is the absolute temperature, R is the universal gas constant (8.314 J/mol/K), and K_{eq} is the standard thermodynamic equilibrium constant of adsorption, M_w (g/mol) is the molecular weight of the absorbate, $C^\circ_{absorbate}$ (mol/L) is the standard concentration of the adsorbate, and $\gamma_{absorbate}$ is the activity coefficient of the adsorbate [37,38].

Table 7 summarizes the thermodynamic parameters for the adsorption of tetracycline on Fe-SiNPs. A negative value of ΔG° indicates a spontaneous adsorption process. The negative ΔS° indicated decreased randomness at solid/solution interface during adsorption [39]. The value of ΔH° was negative, indicating that the adsorption process was exothermic. Molina-Calderón, Basualto-Flores [40] noted that an enthalpy change above 80 kJ/mol (ΔH°>80 kJ/mol) suggests that adsorption process involved chemisorption (surface complexation).

3.10. Adsorption mechanism of TC on Fe-SiNPs

The FTIR spectra of Fe-SiNPs before and after adsorption of TC are

Table 5
Parameters and statistical metrics of adsorption isotherm models for tetracycline adsorption onto Fe-SiNPs at 30 °C, 40 °C, and 50 °C.

Isotherm Model	Temperature		
	30 °C	40 °C	50 °C
Langmuir isotherm model			
Isotherm Constants			
q_m (mg/g)	32.31	65.36	291.70
K_L (L/mg)	0.241	0.097	0.014
Statistical Parameters			
Squared Error	3.04	4.51	1.14
R^2	0.927	0.948	0.988
Freundlich isotherm model			
Isotherm Constants			
K_f (mg/g)	15.32	8.90	4.64
n	5.56	1.80	1.11
Statistical Parameters			
Squared Error	6.93	6.42	1.21
R^2	0.834	0.926	0.987
Temkin isotherm model			
Isotherm Constants			
B_T (J/mol)	11.88	0.71	0.40
A_T (L/mg)	4.82	16.43	26.28
Statistical Parameters			
Squared Error	5.87	4.04	1.72
R^2	0.86	0.954	0.980

Table 6
Maximum tetracycline adsorption capacities for various adsorbents.

Absorbent	q_m (mg/g)	Temperature (°C)	Co (mg/L)	S_{BET} (m^2/g)	Reference
Fe-MSNs	56.98	25	0.005–450	226	[32]
Fe_3O_4/SiO_2/CTAB–SiO_2	220.7	25	25–360	158.4	[33]
Ni-Fe with silica template	90.9	30	–	92	[34]
Amino-Fe(III) functionalized mesoporous silica	23.95	25	0–111	249	[35]
Silica magnetic nanoparticles	61.73	25	20–200	–	[36]
Amino-Fe(III) functionalized SBA15	43.07	25	0–90	245.29	[22]
Fe-SiNPs	65.36	40	90–140	110.83	This study

Co: Initial concentration, S_{BET}: Surface area.

Table 7
Thermodynamic parameters for the adsorption of tetracycline on Fe-SiNPs.

Temperature (K)	K_{eq}	ΔG° (kJ/mol)	ΔH° (kJ/mol)	ΔS° (kJ/mol)	R^2
303.15	107 175.80	−29.19	−114.05	−0.278	0.953
313.15	42 979.88	−27.78			
323.15	6 439.32	−23.56			

presented in Fig. 9. The absorption band observed at 460 – 430 cm^{-1} is attributed to the bending vibration of the Fe–O bond in Fe_2O_3 [41]. The band at 1050 – 990 cm^{-1} and 810 – 790 cm^{-1} are attributed to the antisymmetric and symmetric stretching vibrations of Si–O–Si, respectively [19,41]. The broad absorption band between 3700 and 3000 cm^{-1} corresponds to the stretching vibrations of hydroxyl (–OH) groups [42]. The absorption band 1640 – 1590 cm^{-1} is associated with the stretching vibration of $C = O$ groups [22].

Notably, shifts were observed in the $C = O$ (1640 – 1590 cm^{-1}) and OH (3700 – 3000 cm^{-1}) bands after TC adsorption. According to Zhang, Lan [22], the shift in the $C = O$ band after adsorption (1640 – 1590 cm^{-1}) indicates complexation between TC and Fe(III). Similarly, Bello [43] reported that broadening of the OH group after adsorption signifies hydrogen bonding between the absorbate and adsorbent.

The adsorption thermodynamic studies and the effect of pH suggested that the interaction between TC and Fe-SiNPs involved chemisorption and electrostatic attraction. Consequently, the adsorption mechanism can be attributed to surface complexation (chemisorption), electrostatic attraction, and hydrogen bonding.

4. Conclusions

This study demonstrated that fly ash may be used to synthesise silica nanomaterials that may remove tetracycline from water and/or wastewater. Among the synthesised materials, Fe-SiNPs exhibited the highest TC removal of 59 %, outperforming FA-SiNPs and SSSNPs under identical conditions. The enhanced performance of Fe-SiNPs was attributed to its iron content, which increased the complexation between TC and Fe-SiNPs. The optimal dosage and pHs for TC adsorption using Fe-SiNPs were 5 g/L and pH 4 - 5, respectively. At the optimised dosage and pH, Fe-SiNPs achieved a maximum TC removal of 86 %. The adsorption kinetics of TC on Fe-SiNPs followed the Elovich model, as indicated by the smallest squared error and highest R^2 value. The adsorption isotherms of tetracycline (TC) on Fe-SiNPs were most accurately modelled by the Langmuir isotherm, indicating monolayer adsorption onto a homogeneous surface. Thermodynamic analysis revealed that the adsorption process was endothermic and spontaneous. The overall adsorption mechanism was attributed to chemisorption via surface complexation, electrostatic interactions, and hydrogen bonding. Overall, the findings suggest that Fe-SiNPs presents a viable and sustainable solution for tetracycline removal in water and wastewater treatment. Further work should investigate the development Fe-SiNPs-based beads for application in continuous flow adsorption systems.

Funding

This study was funded by the National Research Foundation (NRF) of South Africa [Grant numbers: CSRP23042396323 and PMDS22062928923].

Conflicts of interest

The authors declare no conflicts of interest. The funders had no role in the design of the study; in the collection, analyses, or interpretation of data; in the writing of the manuscript; or in the decision to publish the results.

CRediT authorship contribution statement

Eric E. Houghton: Data curation, Formal analysis, Methodology, Software, Writing – original draft. **Litha Yapi:** Supervision, Validation, Writing – review & editing. **Shepherd M. Tichapondwa:** Conceptualization, Funding acquisition, Methodology, Supervision, Writing – review & editing.

Declaration of competing interest

The authors declare the following financial interests/personal relationships which may be considered as potential competing interests:

Shepherd Tichapondwa reports financial support was provided by National Research Foundation. Eric Houghton reports financial support was provided by National Research Foundation. If there are other authors, they declare that they have no known competing financial interests or personal relationships that could have appeared to influence the work reported in this paper.

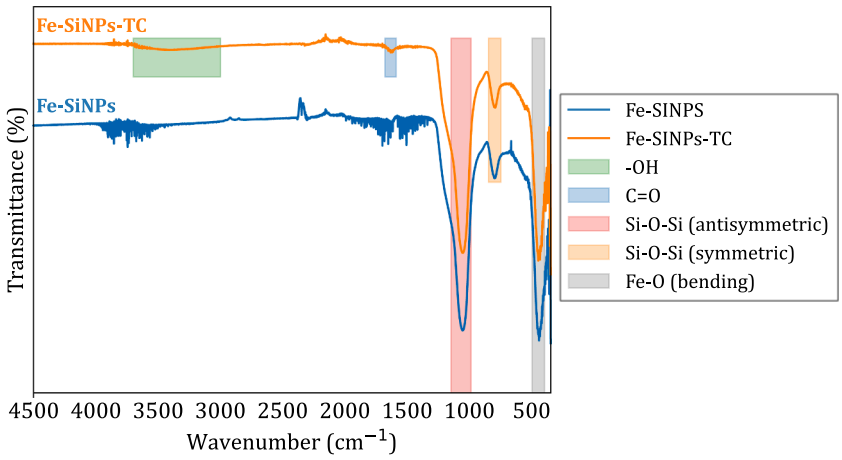

Fig. 9. FTIR spectra of Fe-SiNPs before and after tetracycline (TC) adsorption are presented, with spectra prior to adsorption labelled as Fe-SiNPs and post-adsorption labelled as Fe-SiNPs-TC.

Data availability

Data will be made available on request.

References

[1] G.L. Dotto, G. McKay, Current scenario and challenges in adsorption for water treatment, J. Environ. Chem. Eng. 8 (4) (2020) 103988.
[2] J.X. Loi, et al., Water quality assessment and pollution threat to safe water supply for three river basins in Malaysia, Sci Total Environ. 832 (2022) 155067.
[3] R. Balasubramanian, S. Chowdhury, Graphene-Based 3D Macrostructures for Clean Energy and Environmental Applications, Royal Society of Chemistry (RSC), 2021.
[4] J. Scaria, K. Anupama, P. Nidheesh, Tetracyclines in the environment: an overview on the occurrence, fate, toxicity, detection, removal methods, and sludge management, Sci. Total Environ. 771 (2021) 145291.
[5] J. Antos, et al., Tetracyclines contamination in European aquatic environments: a comprehensive review of occurrence, fate, and removal techniques, Chemosphere 353 (2024) 141519.
[6] Y. Dai, et al., A review on pollution situation and treatment methods of tetracycline in groundwater, Sep. Sci. Technol. 55 (5) (2020) 1005–1021.
[7] R. Vinayagam, et al., Emerging contaminant removal using eco-friendly zinc ferrite nanoparticles: sunlight-driven degradation of tetracycline, Emerg. Contam. 11 (2) (2025) 100469.
[8] Q. Liao, et al., Strong adsorption properties and mechanism of action with regard to tetracycline adsorption of double-network polyvinyl alcohol-copper alginate gel beads, J. Hazard Mater. 422 (2022) 126863.
[9] K. Pyrzynska, Removal of cadmium from wastewaters with low-cost adsorbents, J. Environ. Chem. Eng. 7 (1) (2019) 102795.
[10] R. Chakraborty, et al., Adsorption of heavy metal ions by various low-cost adsorbents: a review, Int. J. Env. Anal. Chem. 102 (2) (2022) 342–379.
[11] A.R.K. Gollakota, V. Volli, C.-M. Shu, Progressive utilisation prospects of coal fly ash: a review, Sci. Total Environ. 672 (2019) 951–989.
[12] Y. Zhang, et al., Treatment of municipal solid waste incineration fly ash: state-of-the-art technologies and future perspectives, J. Hazard Mater. 411 (2021) 125132.
[13] A. Dwivedi, M.K. Jain, Fly ash–waste management and overview: a review, Recent Res. Sci. Technol. 6 (1) (2014) 30–35.
[14] N. Ghazali, K. Muthusamy, S.Wan Ahmad, Utilization of fly ash in construction, in: IOP conference series: materials science and engineering, IOP Publishing, 2019.
[15] P. Ghosh, S. Goel, Physical and chemical characterization of pond ash, Int. J. Environ. Res. Dev. 4 (2) (2014) 129–134.
[16] C. Verma, S. Madan, A. Hussain, Heavy metal contamination of groundwater due to fly ash disposal of coal-fired thermal power plant, Parichha, Jhansi, India, Cogent. Eng. 3 (1) (2016) 1179243.
[17] Q. Guo, et al., Synthesis of disperse amorphous SiO2 nanoparticles via sol–gel process, Ceram. Int. 43 (1) (2017) 192–196.
[18] L.P. Singh, et al., Sol-gel processing of silica nanoparticles and their applications, Adv. Colloid Interface Sci. 214 (2014) 17–37.
[19] P.E. Imoisili, E.C. Nwanna, T.-C. Jen, Facile preparation and characterization of silica nanoparticles from South Africa fly ash using a sol–Gel hydrothermal method, Processes 10 (11) (2022) 2440.
[20] M.E. Aphane, et al., Preparation of sodium silicate solutions and silica nanoparticles from South African coal fly ash, Waste Biomass Valorization 11 (8) (2020) 4403–4417.
[21] M. Manyangadze, et al., Enhancing adsorption capacity of nano-adsorbents via surface modification: a review, S Afr. J. Chem. Eng. 31 (2020) 25–32.
[22] Z. Zhang, et al., Removal of tetracycline antibiotics from aqueous solution by amino-Fe (III) functionalized SBA15, Colloids Surf. A Physicochem. Eng. Asp. 471 (2015) 133–138.
[23] Z. Zhang, et al., Preparation of amino-Fe(III) functionalized mesoporous silica for synergistic adsorption of tetracycline and copper, Chemosphere 138 (2015) 625–632.
[24] E.E. Houghton, et al., Coal fly ash-based adsorbents for tetracycline removal: comparative insights into modification and zeolite conversion, J. Xenobiotics 15 (2) (2025) 36.
[25] P. Kiprono, et al., Iron functionalized silica particles as an ingenious sorbent for removal of fluoride from water, Sci. Rep. 13 (1) (2023) 8018.
[26] G. Nallathambi, et al., Effect of silica nanoparticles and BTCA on physical properties of cotton fabrics, Mater. Res. 14 (2011) 552–559.
[27] I. Gosens, et al., Impact of agglomeration state of nano-and submicron sized gold particles on pulmonary inflammation, Part Fibre Toxicol. 7 (2010) 1–11.
[28] K. Javed, et al., Rice husk ash adsorbent modified by iron oxide with excellent adsorption capacity for arsenic removal from water, Int. J. Environ. Sci. Technol. 20 (3) (2023) 2819–2828.
[29] L. Lohrentz, M. Bhaumik, H.G. Brink, High-capacity adsorption of hexavalent chromium by a polyaniline-Ni(0) nanocomposite adsorbent: expanding the Langmuir-Hinshelwood kinetic model, J. Mol. Liq. 389 (2023).
[30] A.O. Dada, et al., Langmuir, Freundlich, Temkin and Dubinin–Radushkevich isotherms studies of equilibrium sorption of Zn^{2+}unto phosphoric acid modified rice husk, J. Appl. Chem. 3 (2012) 38–45.
[31] M. Aliyu, A.H. Abdullah, M.I.b.M. Tahir, Adsorption tetracycline from aqueous solution using a novel polymeric adsorbent derived from the rubber waste, J. Taiwan Inst. Chem. Eng. 136 (2022) 104333.
[32] H. Qiao, et al., Enhanced sequestration of tetracycline by Mn (II) encapsulated mesoporous silica nanoparticles: synergistic sorption and mechanism, Chemosphere 284 (2021) 131334.
[33] R. Zandipak, S. Sobhanardakani, Novel mesoporous Fe 3 O 4/SiO 2/CTAB–SiO 2 as an effective adsorbent for the removal of amoxicillin and tetracycline from water, Clean Technol. Environ. Policy 20 (2018) 871–885.
[34] X. Wang, et al., Adsorption performance of tetracycline on NiFe layered double hydroxide hollow microspheres synthesized with silica as the template, J. Colloid Interface Sci. 627 (2022) 793–803.
[35] Z. Zhang, et al., Preparation of amino-Fe (III) functionalized mesoporous silica for synergistic adsorption of tetracycline and copper, Chemosphere 138 (2015) 625–632.
[36] N. Farhadian, et al., Removal of tetracycline antibiotic from aqueous environments using core-shell silica magnetic nanoparticles, Desalin. Water Treat. 87 (2017) 348–357.
[37] H.N. Tran, et al., Thermodynamic parameters of liquid–phase adsorption process calculated from different equilibrium constants related to adsorption isotherms: a comparison study, J. Environ. Chem. Eng. 9 (6) (2021) 106674.
[38] S. Raghav, D. Kumar, Adsorption equilibrium, kinetics, and thermodynamic studies of fluoride adsorbed by tetrametallic oxide adsorbent, J. Chem. Eng. Data 63 (5) (2018) 1682–1697.
[39] X. Liu, D.-J. Lee, Thermodynamic parameters for adsorption equilibrium of heavy metals and dyes from wastewaters, Bioresour. Technol. 160 (2014) 24–31.
[40] L. Molina-Calderón, et al., Advances of magnetic nanohydrometallurgy using superparamagnetic nanomaterials as rare earth ions adsorbents: a grand opportunity for sustainable rare earth recovery, Sep. Purif. Technol. 299 (2022) 121708.
[41] P.T.H. Hanh, et al., Adsorption of tetracycline by magnetic mesoporous silica derived from bottom ash—Biomass Power Plant, Sustainability 15 (6) (2023) 4727.
[42] L. Bandura, et al., The role of zeolite structure in its beta-cyclodextrin modification and tetracycline adsorption from aqueous solution: characteristics and sorption mechanism, Materials 15 (18) (2022).
[43] O.S. Bello, Adsorptive removal of malachite green with activated carbon prepared from oil palm fruit fibre by KOH activation and CO2 gasification, S Afr. J. Chem. 66 (2013) 32–41.